C. R. Physique 14 (2013) 531–541

Contents lists available at SciVerse ScienceDirect

Comptes Rendus Physique

www.sciencedirect.com

Trends and perspectives in solid-state wetting / Mouillage solide–solide : tendances et perspectives

Wetting by solid helium, a model system

Mouillage d'une paroi par l'hélium solide, un système modèle

Sébastien Balibar

Laboratoire de physique statistique de l'École normale supérieure, associé au CNRS et aux universités Pierre-et-Marie-Curie & Denis-Diderot, 24, rue Lhomond, 75231 Paris cedex 05, France

ARTICLE INFO

Article history:
Available online 23 July 2013

Keywords:
Nucleation
Metastability
Crystals
Liquids

Mots-clés :
Nucléation
Métastabilité
Cristaux
Liquides

ABSTRACT

This is a review of the wetting properties of solid helium on various solid substrates. Due to its extreme purity and to its very fast growth dynamics, solid helium 4 is often considered as a model system in materials science. Several wetting phenomena have been studied with helium 4 crystals, namely contact angles on solid substrates with variable roughness, wetting on graphite where epitaxial growth takes place, the roughening transition as a function of film thickness, the wetting of grain boundaries by the liquid phase.

RÉSUMÉ

Nous passons en revue les propriétés de mouillage de différents substrats par l'hélium solide. À cause de son extrême pureté et de sa dynamique de croissance très rapide, on considère souvent l'hélium solide comme un système modèle en sciences des matériaux. De nombreux phénomènes de mouillage par l'hélium solide ont été étudiés : angles de contact sur des substrats de rugosité variable, mouillage du graphite où l'on observe une croissance épitaxiale, variation de la transition rugueuse à la surface de films cristallins en fonction de leur épaisseur et mouillage des joints de grains par la phase liquide.

1. Introduction: some peculiarities of solid helium

Solid helium may be considered a model system in materials science [1] for two main reasons: its extreme purity and its fast growth dynamics. In some situations, the quantum properties of solid helium show up but most of the observed phenomena are of universal relevance to classical matter. This is because the large amplitude of the quantum fluctuations has consequences on the phase diagram or on physical quantities like the surface energy, the growth rate or the heat conductivity but, as far as we know at present, there is no macroscopic phase coherence in solid helium that would induce interference effects. Even with superfluid helium actually, the phase coherence intervenes in some rather particular circumstances, but not in wetting properties (except perhaps in the magnitude of Casimir forces determining the thickness of superfluid films adsorbed on a substrate). With helium crystals instead of more usual solids, several phenomena are just observed more simply, more clearly, and more accurately. This is particularly true for the roughening transition of crystal surfaces [2–6,8,9], and for other phenomena like wetting [10,11], nucleation [12–14], stress-induced instability [2,15–22] that is related to the formation of quantum dots in heteroepitaxy [23], and plastic deformation [24]. But the study of solid helium has a cost, namely the necessary use of low-temperature techniques.

E-mail address: balibar@lps.ens.fr.

1631-0705/$ – see front matter
http://dx.doi.org/10.1016/j.crhy.2013.06.002

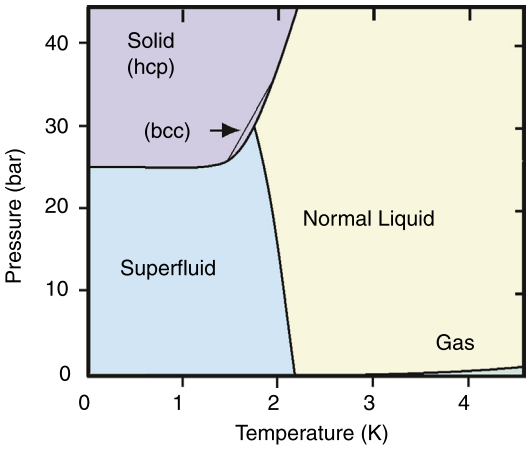

Fig. 1. The phase diagram of ^{4}He. There is no triple point where the gas, liquid and solid phases would meet. Liquid ^{4}He crystallizes above 25.3 bar at low temperature.

Solid helium only exists at pressures higher than 25.3 bar (see the phase diagram in Fig. 1). Under atmospheric pressure, helium liquefies at 4.2 K and at low pressure it stays liquid down to the absolute zero (see Fig. 1). At such temperatures, everything else than helium is frozen and sticks to cell walls. Since liquid helium is superfluid below 2 K and flows very easily through tiny pores, for example Vycor glass where the typical pore diameter is 70 Å, it is easy to filter chemical impurities out. The only impurity in ^{4}He is its light isotope ^{3}He, which is a Fermi particle while ^{4}He is a Bose particle, so that they actually phase separate spontaneously in some part of their phase diagram [25]. The ^{3}He concentration in natural helium is 3×10^{-7} and it can be lowered to 10^{-12} by distillation [26]. Moreover, by using an analog of the "zone melting" method known in metallurgy, it has been shown [25,27] that the ^{3}He concentration can be lowered down to zero in ^{4}He crystals. This is because the liquid–solid equilibrium line extends to $T = 0$ in the phase diagram of helium (Fig. 1). In this review, we consider ^{4}He except if explicitly mentioned.

As shown in Fig. 1, the phase diagram of ^{4}He has no triple point where the gas, the liquid, and the solid phases would meet. As a consequence, He crystals at low temperature are always grown from the liquid phase and the solid–gas interface does not exist. These crystals could be grown at relatively high temperature by cooling down along the melting curve but, below about 1 K, one grows them by pressurizing the liquid. Below 1.78 K, liquid ^{4}He is a superfluid, which implies an absence of viscosity and a large thermal conductivity. Considering that mass and heat transport are easy and that there are no impurities, one may understand that the growth dynamics is very fast, controlled by surface properties, not by bulk diffusion of heat or mass [2,15]. As a result, crystal shapes relax very rapidly to equilibrium so that new, or unconventional methods can be used to measure various surface properties. This is what allowed the roughening of He crystal surfaces to be studied and understood in great details [2–9]. One may also notice on this phase diagram that the melting pressure is nearly temperature independent below 1 K, so that the liquid-to-crystal interface could be studied in a large temperature domain – T can be varied by several orders of magnitude – without changing the pressure significantly.

He atoms are simple with no chemical properties, only a small van der Waals interaction, a hard core repulsion, and some quantum kinetic energy, so that the thermodynamics is very well established. For example, the equation of state of the liquid has been calculated by different methods [14,28–33] that give consistent results, even at negative pressure where the existence of a spinodal limit is well established, in agreement with experimental results on cavitation [12,14]. A spinodal limit has to exist also for the liquid–solid transition, which has been calculated [28,34]. It has been approached in experiments on homogeneous nucleation of crystals [35,36].

At low temperature, ^{4}He crystallization and melting proceed with negligible dissipation and so are very fast: capillary waves can propagate at the liquid–solid interface [2,9]. They were named "crystallization waves" by K.O. Keshishev, who discovered them in 1979 [37]. They involve no significant deformation of the crystal lattice, only local growth and melting. Their careful study has provided an accurate value of the "interfacial energy" also called "interfacial tension" $\alpha(\phi)$, which varies from 0.16 to 0.17 mJ/m^2 as a function of the orientation ϕ of the normal to the interface (see Ref. [2] and references therein). These values correspond to the hexagonal close packed (hcp) phase that is the most studied one. A body centered cubic (bcc) phase exists in a small temperature window between 1.46 and 1.78 K. In their early measurements of capillary depressions, Balibar, Edwards and Laroche [38] found 0.1 mJ/m^2 for the liquid to bcc-solid interfacial energy, but the bcc-solid has been much less studied and, unless explicitly stated, we will consider only the hcp phase in this review. The "interfacial stiffness" $\gamma(\phi) = \alpha + \partial^2\alpha/\partial\phi^2$ of hcp crystals controls the curvature and consequently the equilibrium shape of crystals. It is also known rather accurately [2]. It is obviously important to know both α and its derivatives in order to understand wetting by solid helium.

Another consequence of the fast growth dynamics is that the equilibrium crystal shape is achieved very quickly at low temperature. Since the thermal transport is easy in superfluid helium and actually even larger in helium crystals at low T, the temperature is extremely homogeneous in any cell containing helium crystals in contact with superfluid helium.

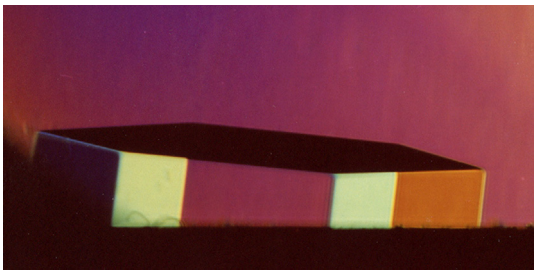

Fig. 2. At low temperature and above 25.3 bar, helium solidifies in the hexagonal compact structure. During fast enough growth from the liquid phase, the crystal shape involves facets, which can be seen in an optical cryostat. Colors corresponding to each couple of facets are obtained by illuminating the crystal with light that is dispersed through a glass prism (see Ref. [2]). The black hexagonal facet on top shows that the 6-fold symmetry axis c of the hcp structure is nearly vertical for this particular crystal. Color available on the web.

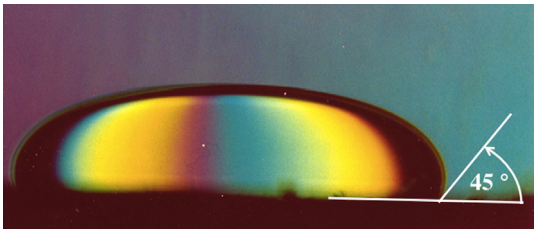

Fig. 3. Sasaki et al. [11] have studied the equilibrium shape of hcp helium crystals on a copper plate. Here, the temperature $T = 1.4$ K is higher than all roughening transition temperatures and the surface is fully rounded, that is rough everywhere. The photograph shows that hcp crystals do not wet this solid surface. There is a partial wetting by the liquid phase with a contact angle of about 45 degrees. Careful studies have shown that this angle depends on whether the contact line advances or recedes. Color available on the web.

As a consequence, gravity and surface stiffness effects drive crystal shapes quickly towards a steady shape. However, the liquid–solid interface may be pinned at various places on the cell walls. This pinning may be avoided by using highly polished walls. Inversely, it can be used to prepare, anchor and study grain boundaries between different crystals.

2. Contact angles

Fig. 3 shows a hexagonal close packed (hcp) He crystal at 1.4 K, in equilibrium with liquid helium above and in contact with a metallic surface below. As for Fig. 2, the colors are obtained by illuminating the experimental cell with white light dispersed with a prism. At this temperature that is higher than all roughening transition temperatures, there are no facets. It is an equilibrium shape and it is flattened by gravity because the size is about 4 mm, that is macroscopic and larger than the capillary length:

$$l_C = \sqrt{\frac{\alpha}{g\delta\rho}} \tag{1}$$

where g is the gravity acceleration and $\delta\rho = (\rho_C - \rho_L)$ is the density difference between the crystal (C) and the liquid (L). As in most systems, the capillary length $l_C \approx 1$ mm. Fig. 3 indicates a contact angle with the solid wall close to 45 degrees, that is partial wetting by the liquid phase. For bcc crystals, the contact angle is similar, about 40 degrees [38]. It means that the crystal-to-solid wall interfacial energy is larger than for the liquid. This non-wetting resembles that of metallic crystallites on a graphite surface as observed by J.-C. Heyraud et al. [39], among others. However, in the latter case, it is probably because the interatomic interaction in the metal is stronger than the metal to graphite interaction. The case of helium must be different. Indeed the solid and the liquid have similar densities and the He–He interaction is weak. The dominant effect must be that the substrate attraction creates strains in the helium crystal so that the He–substrate interfacial energy contains a large elastic term.

As one would write for a liquid–substrate, there is a Young–Dupré equation:

$$\alpha_{CS} - \alpha_{LS} = \alpha_{LC}\cos\theta \tag{2}$$

relating the contact angle θ to the three interfacial energies at play between the crystal (C), the liquid (L) and the substrate (S). For simplicity, we have neglected the anisotropy of the interfacial stiffnesses and replaced them by energies. A rigorous treatment should involve this anisotropy to treat the dependence of the contact angle on the crystal orientation. But the accuracy of Sasaki's measurements was not sufficient for an accurate determination of this dependence. Still, they could study the hysteresis of the contact angle and its dependence on the roughness of the substrate.

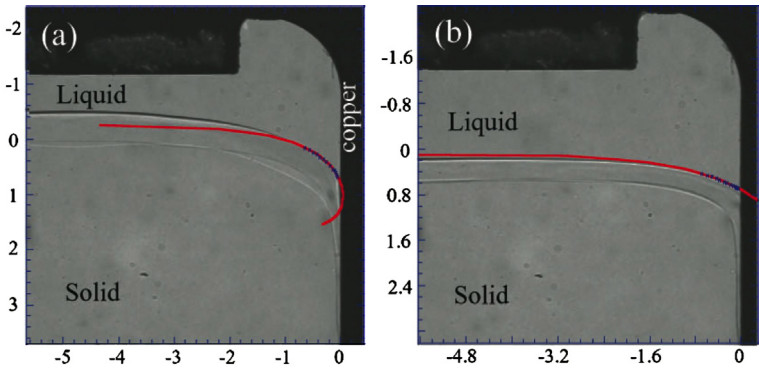

Fig. 4. A helium crystal in contact with a copper wall as studied by Sasaki et al. [11]. Axes are labeled in mm. The photographs were taken at 65 mK: (a) for slow growth at 60 μm/s, and (b) for slow melting at 5 μm/s. Superimposed on the photographs are red solid lines corresponding to the Laplace equation. Color available on the web.

Table 1
Sasaki et al. [11] have shown that even for slow motion (≈ 10 μm/s) of the liquid–solid interface, its contact angle with a copper wall is hysteretic. During growth the angle θ_{adv} is smaller than during melting (θ_{rec}). Missing data correspond to cases where the angle measurement was made difficult by the presence of a facet near the contact line.

	θ_{adv}	θ_{rec}
S4	$22 \pm 2°$	$61 \pm 2°$
S5	$26 \pm 4°$	–
S7	$14 \pm 7°$	$60 \pm 1°$
S8	–	$57 \pm 2°$
S10	–	$48 \pm 6°$
S11	$26 \pm 4°$	$50 \pm 2°$

2.1. Hysteresis of the contact angle

As shown in Fig. 4, the contact angle measured by Sasaki et al. [11] depends on whether the solid–liquid interface advances (during growth) or recedes (during melting). They first measured the contact angle of helium crystals with a copper wall. For this, they fitted the crystal shape with the simplified Laplace equation [40,41]:

$$x = x_0 + l_c \operatorname{arg\,cosh}\left(\frac{2l_c}{z}\right) - 2l_c\sqrt{1 - \frac{z^2}{4l_c^2}} \tag{3}$$

This equation is "simplified" in the sense that the curvature in the vertical plane parallel to the optical axis is assumed to be constant and the true Laplace equation can be integrated once. The fit was made on a small fraction of the meniscus in order to have negligible anisotropy of the interfacial tension. Apparently, the effect of this anisotropy remains small on a large fraction of the interface, since the calculated shape is close to the real shape on a large fraction of the crystal surface.

Sasaki et al. [11] have observed that the advancing contact angle θ_{adv} obtained for slow crystallization is smaller than the receding contact angle θ_{rec} obtained for slow melting (see Fig. 4). Table 1 summarizes angle measurements for six different samples at a typical velocity of 10 μm/s. Sasaki et al. studied different samples with different orientations and the contact angles changed, but θ_{adv} was always smaller than θ_{rec}. They summarized their results with the average values $\theta_{adv} \simeq 22°$ and $\theta_{rec} \simeq 55°$. However, one should keep in mind that the angle values are not randomly scattered: they depend on the crystal orientation, so that it would be meaningless to give an error bar on the average values above.

As for the contact with a glass wall, they observed the same type of behavior, as summarized in Table 2. Apparently, the advancing angle is about 36° and the receding angle is about 51°. If the difference is significant, it shows a slightly smaller hysteresis for glass than for copper. Since their copper walls were not polished after machining, this result would be consistent with the generally accepted idea that the hysteresis is an increasing function of roughness [42].

2.2. Epitaxial growth on graphite

2.2.1. Contact angles with graphite

In 1980, Eckstein [43], followed by Balibar et al. [44], showed that graphite substrates favored the nucleation of oriented helium crystals on their surface. As explained below, J. Maynard and his group demonstrated and further studied the epitaxial growth of ^{4}He crystals on clean graphite substrates [45,46]. A similar epitaxial growth was found for bcc ^{3}He crystals on cubic MgO substrates [43].

Table 2
Hysteresis of the contact angle on a glass wall as measured by Sasaki et al. [11]. The results are similar to the case of a copper wall (Table 1). Here again, the presence of facets sometimes made their measurement impossible.

	θ_{adv}	θ_{rec}
S4	$30 \pm 3°$	$47 \pm 6°$
S5	$30 \pm 8°$	$49 \pm 3°$
S6	–	$53 \pm 2°$
S7	$14 \pm 1°$	$49 \pm 4°$
S8	$33 \pm 5°$	$54 \pm 6°$
S9	$23 \pm 7°$	$61 \pm 5°$
S10	–	$51 \pm 4°$
S11	–	$54 \pm 6°$
S12	–	$51 \pm 4°$
S13	$28 \pm 2°$	$44 \pm 4°$

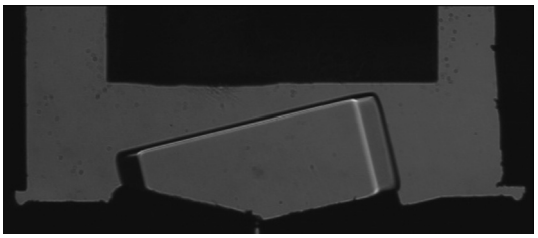

Fig. 5. Nucleation of a helium crystal on a graphite piece, as observed by Sasaki et al. [11]. In this particular case, two pieces of graphite have been glued at the bottom of the cell, forming a V-shape groove. The orientation of the hcp helium crystal is parallel to that of the graphite piece on the right side: its hexagonal *c* facet is parallel to the surface of the graphite.

Sasaki et al. [11] further studied the nucleation of He crystals on graphite substrates. For this, they glued highly oriented pyrolytic graphite (HOPG) and papyex pieces in their cell. The pieces were freshly cleaved but exposed to air during the mounting of the cell. After closure the cell was warmed up to 100 °C and flushed a dozen of times with clean helium gas. This was not sufficient to obtain crystal nucleation on the graphite. In the old experiment by Balibar et al. [44], the graphite was taken to high temperature (about 1000 K) under vacuum by passing a large current through it. In Sasaki's cell, this could not be done. They measured contact angles on these partially cleaned graphite pieces which were similar to what was found on copper and on glass: the advancing angle was between 31° and 43° and the receding angle between 44° and 62°. To obtain nucleation of oriented helium crystals on graphite substrates, it appeared better to pump for three days on the cell at 100 °C without flushing, in which case they observed the desired nucleation of oriented crystals (see Fig. 5). However, the nucleation did not always take place there, indicating that the degassing was probably not yet sufficient. As for the contact angle on graphite, it was again of the order of 45°, except of course when the crystal orientation was parallel to that of the graphite. In fact, when helium crystals are not oriented parallel to the graphite, and since the graphite surface is probably covered by a thin solid helium layer, one expects the contact angle of the liquid–solid interface to be comparable to the groove angle of the grain boundary between two misoriented crystals, i.e. 30° (see below).

2.2.2. Solid films grown on graphite: roughening and layering transitions

Ramesh et al. [45,46] measured the adsorption of solid helium films on graphite. They studied the shape of the adsorption isotherms as a function of temperature. At high enough temperatures, the coverage is a continuous function of pressure P. As P approaches the equilibrium pressure P_{eq}, the coverage increases; it shows structures, but it evolves continuously. At low temperatures, on the contrary, the isotherms show jumps in thickness, which are first-order transitions between films with integer numbers of atomic layers (see Fig. 6). Each of these "layering transitions" has a critical temperature T_{cn}, which depends on the number n of layers. This phenomenon is similar to the roughening transitions [2] of bulk crystals to which it was related by Huse [47] and by Nightingale [48]. For bulk crystals as for thin solid films, the surface may be localized on lattice planes or free to occupy any position in space. For bulk crystals, the surface is localized if the lattice potential is stronger than thermal fluctuations. For thin films, the attractive potential from the substrate has to be considered. It reduces the amplitude of thermal fluctuations, the transition temperature is reduced and the universality class of the transition changed. For the first layer, for example, the attraction is so strong that atoms can be in the first or in the second layer only. In this case, the system is strictly equivalent to the 2D Ising model, with a second-order phase transition, not with a Kosterlitz–Thouless one as for the roughening transition [2]. As the film thickness increases, fluctuations feel a weaker and weaker van der Waals attraction and the critical layering transition should evolve into the roughening transition. More precisely, Huse and Nightingale et al. predicted that T_{cn} tends linearly to T_R as a function of $[\ln n]^{-2}$, where n is the number of atomic layers. This prediction was qualitatively verified by Ramesh et al. [46] at a

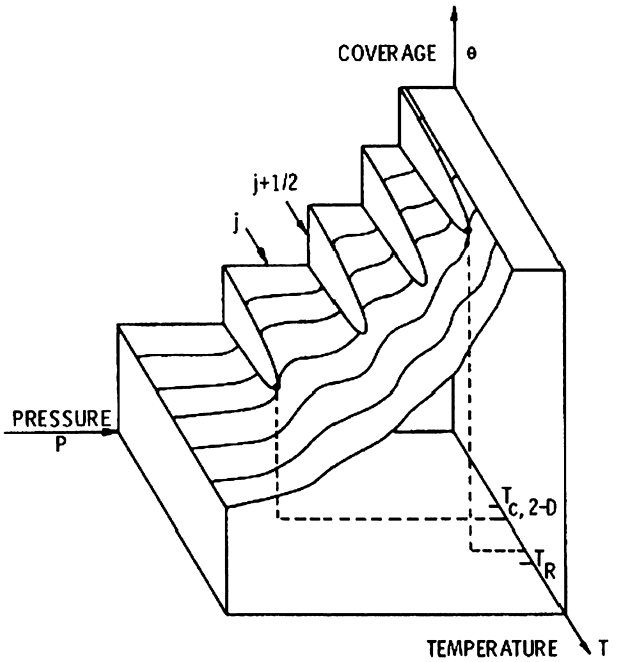

Fig. 6. Adsorption isotherms of solid ^{4}He on graphite from Ramesh et al. [46]. At low temperature, the coverage shows jumps, that is first-order transitions, between successive layers indexed with the integer number j by Ramesh et al. The first-order transitions have critical end points at successive temperatures T_c that depend on the number of atomic layers.

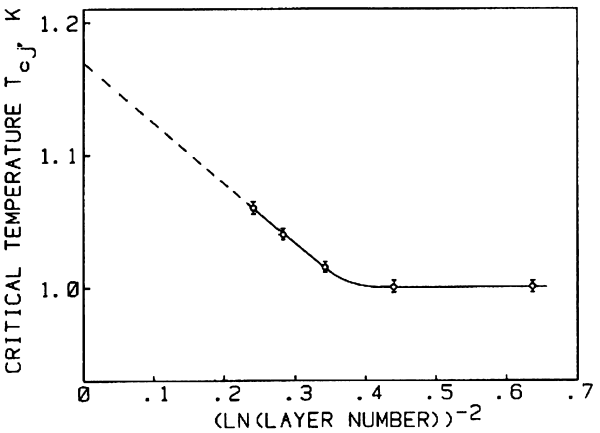

Fig. 7. Extrapolation by Ramesh et al. [46] of the critical layering transition temperatures $T_c(n)$ in ^{4}He as a function of the number n of layers, more precisely $(\ln n)^{-2}$. According to Huse [47] and Nightingale et al. [48], T_c tends to the roughening temperature T_R at infinite thickness.

time when the roughening transition temperature of ^{4}He crystals was not yet accurately known. It has been shown to be 1.30 K [2] not 1.17 K, as suggested by the extrapolation in Fig. 7. It would be very interesting to extend Ramesh's measurements beyond eight layers, the maximum thickness in Ramesh's experiment, in order to obtain a better check of this prediction.

Later the same group [49] discovered a surprising phenomenon. As temperature was lowered below 0.5 K, their fourth sound measurement technique showed the existence of a feature at a half-filling of solid ^{4}He layers. It seems that layers are being completed in two stages, not in a single one as was expected before. They first proposed to relate this observation to the existence of quantum kinks whose mobility drastically changes when thermal rotons disappear or when ^{3}He impurities adsorb on the steps. They suggested another possible interpretation, namely that some reconstruction of the (0001) surface could occur if one forces a half-filling of layers. Such ideas were also proposed by Gridin et al. [50], who observed similar features in their adsorption isotherms. The whole issue is interesting and undecided yet.

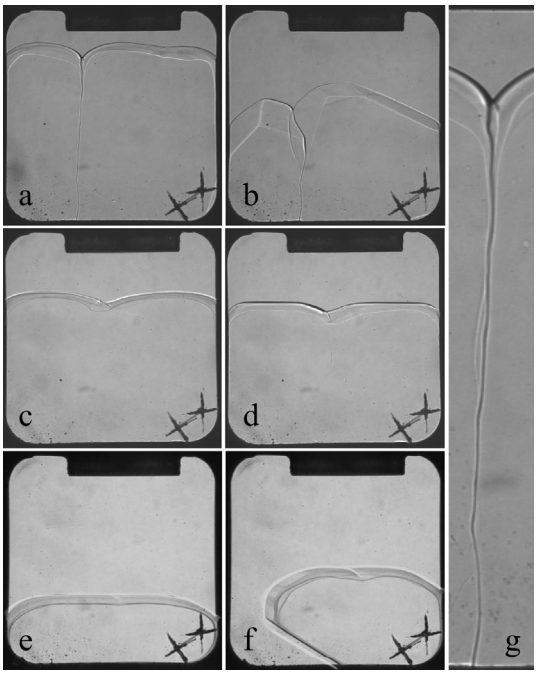

Fig. 8. Three pairs of images obtained by Sasaki et al. [11] showing equilibrium shapes (a, c, e) together with growth shapes that reveal the crystal orientation (b, d, f). When the two crystal grains have a large difference in orientation (a, b), their boundary ends as a deep groove at the liquid–solid interface. A zoom of (a) shows that the contact lines of the GB with the windows are in fact liquid channels (g). Crystals with similar orientations can be obtained by direct growth (c, d, e, f). In this case, the groove is shallow with no liquid channels on the windows. Two crosses carved on the windows help adjusting the focusing.

3. Wetting of grain boundaries

3.1. Preparation of grain boundaries

Sasaki et al. [11] used the fast growth dynamics of helium crystals to prepare grain boundaries (GB) whose energy could be measured. They started with a polycrystal grown at constant volume from normal liquid He or by fast pressurization at low temperature. When removing helium from the cell through its fill line, a macroscopic liquid phase appeared at the melting pressure. At that time, they observed a quick Ostwald ripening that is a consequence of capillary effects with the liquid phase, allowing fast mass transport from small crystals that melt to larger crystals, which grow. In reality, the crystals that melt are those which are smaller than the capillary length $l_C \approx 1$ mm, so that their surface shows a definite curvature.

In the end, they were usually left with a few crystals larger than l_C. With a thin cell, the GBs are oriented nearly perpendicular to the windows. This occurs for capillary reasons, like in a soap foam between two plates: interfaces perpendicular to the walls have a smaller area. In order to keep only two grains, they had to remove some more helium. If this was done slowly enough, the smallest crystals melted one after the other until only two were left. At this stage, they could grow them again, to form a large bi-crystal with only one GB, which is rather stable in time (see Fig. 8). They could align the GB close to the vertical direction using successive growth and melting cycles. If needed, they could finally adjust the optical axis precisely parallel to the GB plane by moving their camera.

Before considering the grain boundaries in more details, it might be useful to note that two crystals prepared with exactly the same orientation should of course coalesce when they touch each other, and make one single crystal. This has been observed very clearly and the coalescence dynamics studied with bcc helium 3 crystals [51]. However, with hcp helium 4 crystals, the coalescence is very much faster and difficult to analyze, because helium 4 is superfluid, but not helium 3, at easily accessible temperatures. Furthermore, it is difficult to avoid the presence of stacking faults, which prevent coalescence of hcp crystals.

3.2. The grain boundary energy

Fig. 8 shows three examples of ^{4}He bi-crystals obtained by Sasaki et al. [11]. The pictures (b), (d), (f) show growth shapes corresponding respectively to the equilibrium shapes (a), (c), (e). The growth shapes reveal facets, and one can see that the pictures (a), (b) correspond to a GB between two grains with rather different orientations. The picture (g) is an enlargement of the GB seen on picture (a).

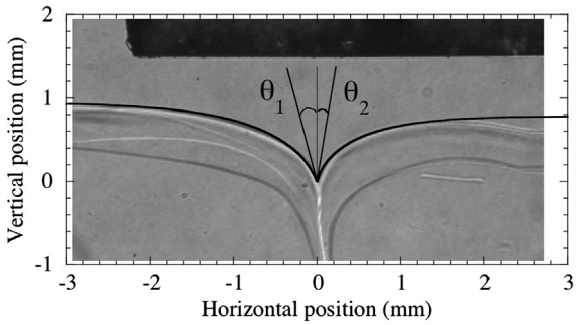

Fig. 9. The dihedral angle $2\theta = \theta_1 + \theta_2$ is determined by fitting each crystal profile with the Laplace equation near the groove.

Table 3
The dihedral angle $2\theta = \theta_1 + \theta_2$ of grain boundaries, as measured with three different samples (S1, S2, S3) by Sasaki et al. [11].

Sample	Angles (°)			Surface energies (mJ/m^{-2})		
	θ_1	θ_2	2θ	α_1	α_2	α_{GB}
S1	20.3	1.8	22.1	0.113	0.0800	0.186
S2	20.0	12.4	32.4	0.0985	0.0674	0.158
S3	14.8	14.2	29	0.0555	0.0823	0.133

As explained in Ref. [10], GBs emerging at the liquid–solid interface make a groove to reach the mechanical balance between the GB surface tension α_{GB} and the liquid–solid interfacial tension α_{LS}. In a first approximation, $\alpha_{GB} = 2\alpha_{LS}\cos\theta$, where 2θ is the dihedral angle of the groove. However, since the two crystals have different orientations, the liquid–solid interface makes an angle θ_1 with the vertical on the left (crystal 1) and an angle θ_2 on the right (see Fig. 9). As a consequence, a more rigorous expression is:

$$\alpha_{GB} = \alpha_1 \cos\theta_1 + \alpha_2 \cos\theta_2 \tag{4}$$

Furthermore, since the GB is not strictly vertical, the above equation is slightly incorrect with $\theta_{1,2}$ measured from the vertical. However, Sasaki et al. [11] verified that the corresponding error on the measurement of α_{GB} is around 0.5%, that is small compared to their final error bar (±2%). The definition of angles and Eq. (4) could be kept for simplicity with a dihedral angle $2\theta = \theta_1 + \theta_2$.

For three examples of crystals like (8a), the groove is deep with sharp but non-zero angles (see below). When trying to grow the solid by directly pressurizing the superfluid, one usually ends with a single crystal. However, Sasaki et al. [11] could also produce two crystals with similar orientations (Figs. 8c, d, e, f), in which case the groove is shallow, indicating a GB with small α_{GB}, perhaps a stacking fault. This interpretation would be consistent with the measurements by Junes et al. [52].

In order to make a precise measurement of the groove angles, Sasaki et al. used a fit with a Laplace equation where the surface tension and the angle were adjustable parameters. They assumed that the curvature in the plane perpendicular to the windows was approximately constant, so that they used the simplified version of the Laplace equation (Eq. (3)).

Since the surface tension is known to be anisotropic for hcp helium 4 crystals [2], the fit was made on a small part of the meniscus (about 2.5 mm long) on each side of the groove. Fig. 9 shows that the result is close to the real meniscus, even far away from the groove, meaning that, in this particular case, the anisotropy of the surface stiffness was not very large. Table 3 gives the results corresponding to three pairs of crystals (S1, S2, and S3).

In the end, Sasaki et al. found that the dihedral angle of the groove $(\theta_1 + \theta_2)$ is strictly positive, in the order of 30°. The GB energy is of order 0.15 mJ/m^2, strictly less than $\alpha_1 + \alpha_2$. They were primarily interested in measuring the dihedral angle, for which the above procedure was sufficient. The good quality of their fit away from the groove explains why the use of an integrated version of Eq. (3):

$$(\rho_S - \rho_L)\, g\, (\Delta z)^2 = 2\,\alpha_{LS}\,(1 - \sin\theta) \tag{5}$$

gave them similar values for θ (Δz is the depth of the groove). Eq. (5) is similar to one widely used to determine the liquid–solid surface tension of classical systems, in experiments where gravity is replaced by a temperature gradient [53,54].

The physical meaning of Sasaki's measurements is that, even at the liquid–solid equilibrium, a GB is not completely wet by the liquid phase. Complete wetting ($\theta = 0$) would imply the invasion of the grain boundary by a liquid region of macroscopic thickness, the grain boundary would be simply made of two liquid–solid interfaces and α_{GB} would be equal to $2\alpha_{LS}$. Sasaki's measurement of a non-zero cusp angle demonstrates that the grain boundary is a thin object of microscopic thickness. This is consistent with the numerical simulations by Pollet et al. [55], who showed that GBs are generally made of three disordered layers of atoms. The wetting of GBs is an important issue in materials science.

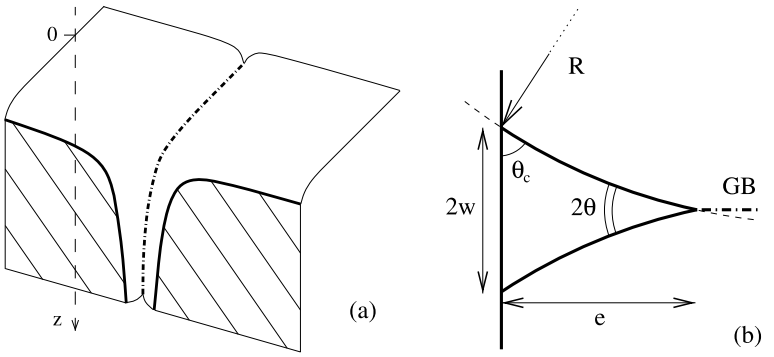

Fig. 10. (a) Three-dimensional view of the contact between a grain boundary (dash-dotted line) and a wall [10]. The hatched area shows the contact of the wall with the solid. (b) Horizontal cross section of the liquid channel near the wall.

It has even been predicted that GBs could premelt [56], that is melt before the bulk, being invaded by a thick liquid layer at a temperature below the bulk melting temperature T_m. However, experimental evidence is rather difficult to obtain. Hsieh and Balluffi studied aluminum films, and concluded that "no complete grain boundary melting was detectable by local diffraction contrast at temperature lower than $0.999\,T_m$" [57]. GB premelting has been reported in colloidal crystals, but only above $0.999T_m$ [58]. In fact, although premelting is possible in systems with short-range forces, it cannot happen in the case of long-range forces (e.g., van der Waals forces) [59–61]. More details could be found in Ref. [62].

Franck et al. [63,64] studied thin films (less than 50 μm thick) of fcc helium at high pressure and temperature. Their observation technique used a Schlieren method that did not allow them to measure precisely the dihedral angle; they were only able to state that $0 \leqslant 2\theta \leqslant 30°$. Their experiment is sometimes erroneously interpreted as evidence for complete wetting [65]. In fact, because the films lie on a sapphire substrate favorable to the liquid, we shall see below that, where they touch a sapphire window, GBs open up as macroscopic liquid channels for simple reasons having to do with the equilibrium of local surface tensions. Sasaki et al. [11] explained that Franck observed these liquid channels near the sapphire surface, not the wetting of the grain boundaries in the bulk of the crystals.

4. Contact lines of grain boundaries

4.1. Liquid channels along walls

As shown in Figs. 8a, b and g, a liquid channel can exist at the contact line between the GB and the glass window of the cell. As explained in Ref. [10], this phenomenon is due to the glass wall being preferentially wet, although not completely, by the liquid phase. It occurs when the GB energy α_{GB} is large enough.

Fig. 10a shows a schematic view of a liquid channel. Its existence is a consequence of gravity, hydrostatic equilibrium, and force balance on contact lines.

The width of the liquid channel decreases rapidly when the solid pressure P_S increases above the liquid–solid equilibrium pressure P_{eq}. The typical pressure at which it closes is when this width reaches 1 nm, the typical thickness of a GB. This was found to occur 1 MPa above P_{eq} in the case of helium, except if important stress gradients take place in the solid.

A similar phenomenon occurs if three crystal grains meet. They define three GBs that meet at a contact line. For the same reason as that considered above, this contact line will be invaded by the liquid phase if the groove angle is less than 60°, as is the case in helium.

A polycrystal near P_{eq} should thus be invaded by a three-dimensional network of liquid channels. This effect had already been predicted by Miller and Chadwick [66], who expressed the departure from the melting curve in terms of temperature instead of pressure, but this is equivalent. Such a network has been observed in ice crystals [67]. Each node of this network will be a liquid droplet. If the pressure increases above P_{eq}, the channels and droplets will shrink and close around 1 MPa above P_{eq} when their size becomes of atomic dimension, unless they are stabilized by local stresses, as already mentioned.

5. Conclusion

In this review, I have described some wetting phenomena that have been observed with helium crystals in contact with solid walls. None of them is particular to quantum crystals. In reality, they illustrate the general laws governing wetting in classical systems. It is only the values of some parameters like the surface energy or stiffness of crystals, which are a little different from what is known in classical solids. And, of course, the growth dynamics of helium crystals allows unconventional methods to be used to study wetting phenomena.

I have focused on some properties that are directly related to wetting. I could have described an important mechanical instability that occurs when a non-hydrostatic stress is applied to crystals. This instability is known as the "Asaro–Tiller–Grinfeld" instability, from the names of the three authors of pioneering work on it [16–18]. It has been shown

experimentally that when a horizontal stress is applied to a helium crystal in equilibrium with superfluid helium above, regularly spaced grooves appear beyond a critical stress σ_C [19–21], in agreement with developments of the theory of this instability [2,15,22]. The physical interpretation of this instability is that a modulation of the height of the crystal surface allows some release of elastic energy at the expense of some surface energy. A clear relation of this phenomenon to wetting has been made by J.N. Aqua et al. [23]. The same instability occurs in heteroepitaxy of semiconductors where a lattice mismatch between layers of different materials – for example Ge on Si or AlGaAs on GaAs – produces an anisotropic strain and most importantly the formation of quantum dots, which are very well known for their use in modern technology. There is a difference in scale because, in helium, one observed the formation of grooves separated by millimeters at the critical stress while, in semiconductors, the stress is very much larger, so that the wavelength of the instability is in the nanometer range. But it is now understood that the origin of the instability is the same. Future experiments could fill the gap between the two scale domains.

Another phenomenon has not been described in this review, namely the crystallization of helium inside porous media, on which interesting work is done by the group of Y. Okuda [68]. In conclusion, some more work with solid helium might further improve our understanding of wetting by solids.

Acknowledgement

I acknowledge support from ERC grant AdG 247258-SUPERSOLID.

References

[1] S. Balibar, P. Nozières, Solid State Commun. 92 (1994) 19.
[2] S. Balibar, H. Alles, A.Ya. Parshin, Rev. Mod. Phys. 77 (2005) 317.
[3] S. Balibar, B. Castaing, J. Phys. Lett. 41 (1980) 329.
[4] P.E. Wolf, S. Balibar, F. Gallet, Phys. Rev. Lett. 51 (1983) 1366.
[5] P.E. Wolf, F. Gallet, S. Balibar, E. Rolley, P. Nozières, J. Phys. 46 (1985) 1987.
[6] F. Gallet, P. Nozières, S. Balibar, E. Rolley, Europhys. Lett. 2 (1986) 701.
[7] E. Rolley, S. Balibar, F. Gallet, Europhys. Lett. 2 (1986) 247.
[8] F. Gallet, S. Balibar, E. Rolley, J. Physique 48 (1987) 369.
[9] E. Rolley, C. Guthmann, E. Chevalier, S. Balibar, J. Low Temp. Phys. 99 (1995) 851.
[10] S. Sasaki, F. Caupin, S. Balibar, Phys. Rev. Lett. 99 (2007) 205302.
[11] S. Sasaki, F. Caupin, S. Balibar, J. Low Temp. Phys. 153 (2008) 43.
[12] S. Balibar, J. Low Temp. Phys. 129 (2002) 363.
[13] S. Balibar, F. Caupin, C. R. Physique 7 (2006) 988.
[14] F. Caupin, S. Balibar, Phys. Rev. B 64 (2001) 064507.
[15] S. Balibar, D.O. Edwards, W.F. Saam, J. Low Temp. Phys. 82 (1991) 119.
[16] R.J. Asaro, W.A. Tiller, Metall. Trans. A 3 (1972) 1789.
[17] M.A. Grinfeld, Dokl. Akad. Nauk SSSR 290 (1986) 1358, Sov. Phys. Dokl. 31 (1986) 831.
[18] M.A. Grinfeld, J. Nonlinear Sci. 3 (1993) 35.
[19] R. Torii, S. Balibar, J. Low Temp. Phys. 89 (1992) 391.
[20] J. Bodensohn, K. Nicolai, P. Leiderer, Z. Phys. B: Condens. Matter 64 (1986) 55.
[21] M. Thiel, A. Willibald, P. Evers, A. Levchenko, P. Leiderer, S. Balibar, Europhys. Lett. 20 (1992) 707.
[22] P. Nozières, Shape and growth of crystals, in: C. Godrèche (Ed.), Solids Far from Equilibrium, Cambridge University Press, UK, 1992.
[23] J.N. Aqua, T. Frisch, A. Verga, Phys. Rev. B 76 (2007) 165319.
[24] A. Haziot, X. Rojas, A.D. Fefferman, J. Beamish, S. Balibar, Phys. Rev. Lett. 110 (2013) 035301.
[25] D.O. Edwards, S. Balibar, Phys. Rev. B 39 (1989) 4083.
[26] P.V.E. McClintock, Cryogenics 18 (1978) 201.
[27] C. Pantalei, X. Rojas, D.O. Edwards, S. Balibar, J. Low Temp. Phys. 159 (2010) 452.
[28] H.J. Maris, F. Caupin, J. Low Temp. Phys. 131 (2003) 145.
[29] H.J. Maris, J. Low Temp. Phys. 94 (1994) 125.
[30] H.J. Maris, J. Low Temp. Phys. 98 (1995) 403.
[31] M. Guilleumas, M. Pi, M. Barranco, J. Navarro, M.A. Solis, Phys. Rev. B 47 (1993) 9116.
[32] M.A. Solís, J. Navarro, Phys. Rev. B 45 (1992) 13080.
[33] J. Casulleras, J. Boronat, Phys. Rev. Lett. 84 (2000) 3121.
[34] L. Vranjes, J. Boronat, J. Casulleras, C. Cazorla, Phys. Rev. Lett. 95 (2005) 145302.
[35] F. Werner, G. Beaume, A. Hobeika, S. Nascimbene, C. Herrmann, F. Caupin, S. Balibar, J. Low Temp. Phys. 136 (2004) 93.
[36] R. Ishiguro, F. Caupin, S. Balibar, Europhys. Lett. 75 (2006) 91.
[37] K.O. Keshishev, A.Y. Parshin, A.V. Babkin, Pis'ma Zh. Eksp. Teor. Fiz. 30 (1979) 63, JETP Lett. 30 (1980) 56.
[38] S. Balibar, D.O. Edwards, C. Laroche, Phys. Rev. Lett. 42 (1979) 782.
[39] J.-C. Heyraud, J.-J. Metois, Surf. Sci. 128 (1983) 334;
C. Rottman, M. Wortis, J.-C. Heyraud, J.-J. Metois, Phys. Rev. Lett. 52 (1984) 1009.
[40] L.D. Landau, I.M. Lifshitz, Fluid Mechanics, Theoretical Physics, vol. 6, Pergamon Press, 1959, Chapter VII.
[41] P.-G. de Gennes, F. Brochard-Wyart, D. Quéré, Capillarity and Wetting Phenomena: Drops, Bubbles, Pearls, Waves, Springer, 2003, Chapter 2, Section 3.2.
[42] E. Rolley, C. Guthmann, Phys. Rev. Lett. 98 (2007) 166105.
[43] Y. Eckstein, J. Landau, S.G. Lipson, Z. Olami, Phys. Rev. Lett. 45 (1980) 1805.
[44] S. Balibar, B. Castaing, C. Laroche, J. Phys. Lett. 41 (1980) 283.
[45] S. Ramesh, J.D. Maynard, Phys. Rev. Lett. 49 (1982) 47.
[46] S. Ramesh, Q. Zhang, G. Torzo, J.D. Maynard, Phys. Rev. Lett. 52 (1984) 2375.
[47] D.A. Huse, Phys. Rev. B 30 (1984) 1371.
[48] P.M. Nightingale, W.F. Saam, M. Schick, Phys. Rev. B 30 (1984) 3830.

[49] M.J. McKenna, T.P. Brosius, J.D. Maynard, Phys. Rev. Lett. 69 (1992) 3346.
[50] V. Gridin, J. Adler, Y. Eckstein, E. Polturak, Phys. Rev. Lett. 53 (1984) 802.
[51] R. Ishiguro, F. Graner, E. Rolley, S. Balibar, Phys. Rev. Lett. 93 (2004) 235301.
[52] H.J. Junes, H. Alles, M.S. Manninen, A.Ya. Parshin, I.A. Todoshchenko, J. Low Temp. Phys. 153 (2008) 244.
[53] G.F. Bolling, W.A. Tiller, J. Appl. Phys. 31 (1960) 1345.
[54] U. Boyuk, K. Keslioglu, N. Marash, J. Phys.: Condens. Matter 19 (2007) 116202, and references therein.
[55] L. Pollet, M. Boninsegni, A.B. Kuklov, N.V. Prokof'ev, B.V. Svistunov, M. Troyer, Phys. Rev. Lett. 98 (2007) 135301.
[56] R. Kikuchi, J.W. Cahn, Phys. Rev. B 21 (1980) 1893.
[57] T.E. Hsieh, R.W. Balluffi, Acta Metall. 37 (1989) 1637.
[58] A.M. Alsayed, M.F. Islam, J. Zhang, P.J. Collings, A.G. Yodh, Science 309 (2005) 1207.
[59] S. Dietrich, Wetting phenomena, in: C. Domb, J.L. Lebowitz (Eds.), Phase Transitions and Critical Phenomena, vol. 12, Academic Press, 1988, p. 1.
[60] M. Schick, Wei-Heng Shih, Phys. Rev. B 35 (1987) 5030.
[61] R. Lipowsky, Phys. Rev. Lett. 57 (1986) 2876.
[62] F. Caupin, S. Sasaki, S. Balibar, J. Phys.: Condens. Matter 20 (2008) 494228.
[63] J.P. Franck, K.E. Kornelsen, J.R. Manuel, Phys. Rev. Lett. 50 (1983) 1463.
[64] J.P. Franck, J. Gleeson, K.E. Kornelsen, J.R. Manuel, K.A. McGreer, J. Low Temp. Phys. 58 (1985) 153.
[65] J.G. Dash, H.Y. Fu, J.S. Wetlaufer, Rep. Prog. Phys. 58 (1995) 115;
J.G. Dash, J.S. Wetlaufer, Phys. Rev. Lett. 94 (2005) 235301.
[66] W.A. Miller, G.A. Chadwick, Acta Metall. 15 (1967) 607.
[67] A.W. Rempel, E.D. Waddington, J.S. Wettlaufer, M.G. Worster, Nature 411 (2001) 568.
[68] R. Masumoto, K. Ueno, H. Matsuda, et al., J. Low Temp. Phys. 162 (2011) 399.